Controlled Aggregation of Colloidal Particles for Toner Applications

Alyson J. Turner,[1] Smitha Nair,[1] Zhen Lai,[2] Chieh-Min Cheng,[2] Surita R. Bhatia[1]

[1]*Department of Chemical Engineering, University of Massachusetts Amherst, Amherst, Massachusetts 01003*
[2]*Xerox Corporation, 800 Phillips Road, Webster, New York 14580*

Received 17 March 2010; accepted 21 December 2010
DOI 10.1002/app.34018
Published online 23 May 2011 in Wiley Online Library (wileyonlinelibrary.com).

ABSTRACT: Micrometer-sized particles were formed by controlled aggregation of carboxylated polystyrene colloidal spheres having a mean diameter of about 200 nm with a commercial cationic coagulant. To identify the parameters governing the size and structure of the aggregates, the aggregate size distribution was studied over a period of time with dynamic light scattering. The effect of the particle concentration, pH, and ionic strength on the aggregation behavior was investigated. The coagulant concentration used for present studies was 5 parts per hundred on the basis of the polystyrene particles and the particle concentrations used were 10–15%. The particle size distribution for the latex suspensions was also investigated with a 10% aluminum sulfate [$Al_2(SO4)_3{\cdot}14H_2O$] solution as a model coagulant. With the commercial coagulant, aggregation was found to be slower at lower pH than at neutral pH. At pH 6, the particles started to aggregate within minutes and form aggregates of about 1000 nm. We expected that lowering the pH would reduce interparticle repulsive forces and enhance the collision efficiency. However, at a lower pH of 2, the aggregation process slowed down. Increasing the ionic strength at neutral pH led to a broader aggregate size distribution, and the population of larger aggregates increased. The suspensions with the model coagulant showed similar behavior. © 2011 Wiley Periodicals, Inc. J Appl Polym Sci 122: 1358–1363, 2011

Key words: colloids; light scattering; microstructure; nanoparticle; particle size distribution

INTRODUCTION

The quality of digital printing is dependent in part upon the physical properties of the toner particles.[1] Desirable attributes include a mean particle size in the range of 3–9 μm, a narrow particle size and shape distribution, and a homogeneity of composition. The two general methods currently being used to make toners are the conventional mechanical toner manufacturing method, and the chemically processed toner (CPT) method. In the conventional method, a large solid mass of toner is fractured and ground to a fine powder by the milling process, which results in a broad particle size distribution. The variations in particle shape cause a difference in the charge-to-mass ratio. Another disadvantage is the creation of dust. A narrow size distribution can be achieved by air classification; however, it reduces the yield.[1,2]

In the CPT processes, the desired particle size distribution can be achieved, and milling and classification can be avoided. CPT processes can produce toner particles that are smaller with narrower particle size and shape distributions. This CPT process involves the production of latex precursor particles (~ 200 nm) by emulsion polymerization. After the optional addition of pigments or additives, the particles are then flocculated, usually by adjustment of the pH.[3,4] The resulting gel, with a branched, networklike structure, is mechanically agitated to break up the network into microsized toner particles. The temperature can be adjusted during or after this process to promote fusion of the precursor particles into a homogeneous larger particle.[4] Ding et al. studied the microstructure and rheological properties during the pH and temperature changes associated with the manufacture of a chemically produced toner[3] and the details of the process and hydrodynamic conditions, which precisely affected the size distributions of the final toner particles.[4] More recently, an improved CPT process, known as the *emulsion–aggregation (EA) toner process*, has been developed.[5,6] The EA process employs the use of specific coagulating agents to better control the aggregation step. The process results in dense aggregates and avoids the formation of a viscous gel phase. The EA process has the advantage of improved control over the polydispersity and size of the toner particles.[6]

In a typical CPT process, carboxy-functionalized colloids are used as the primary particles.[3] At neutral pH, the primary particles are charge-stabilized.

Correspondence to: S. R. Bhatia (sbhatia@ecs.umass.edu).

As the pH is lowered, the carboxyl groups revert from charged to nonionic, and the particles quickly aggregate to form a fractal gel. The aggregate is infinite in size in such systems; it will continue to grow until it either precipitates out of solution or spans the entire system, forming a gel. There have been several fundamental experimental and theoretical studies of similar colloidal aggregation processes and the rheology and structure of the resulting fractal colloidal gels.[7–12] By contrast, there have been fewer studies on the dense colloidal aggregates that appear to be formed by the EA process. Stable, finite-sized dense clusters have been observed in attractive colloids with long-range electrostatic repulsions,[13] although more recent work suggests that dense clusters may also form in systems with moderate-range attractions, even in the absence of long-range repulsion.[14] In these types of systems, the role of factors such as pH and ionic strength on the aggregation process and aggregate size are unclear.

In this study, we investigated two systems that serve as models for the EA process. Micrometer-sized particles were formed by the controlled aggregation of carboxylated polystyrene colloidal spheres ($\sim$ 200 nm) in the presence of a commercial cationic coagulant and a model coagulant. The particle size and particle size distribution were studied over a period of time with dynamic light scattering. The effects of the particle concentration, pH, and ionic strength on the aggregation behavior were investigated.

EXPERIMENTAL

Materials

A latex suspension of carboxylated polystyrene particles, with a solid content of 41 wt % and a particle size (mean diameter) of about 200 nm, and a commercial cationic coagulant were obtained from Xerox Corp. (Webster, NY) Hydrated aluminum sulfate [$Al_2(SO4)_3{\cdot}14H_2O$] obtained from Sigma Aldrich was used as the model coagulant.

Sample preparation

The latex suspension was diluted to 10 or 15 wt % solids with nanopure water. To these suspensions, 5 parts per hundred (pph) of cationic coagulant per primary particle was added. Two sets of samples at low pH were prepared, one in which the pH was adjusted with buffer and one in which hydrochloric acid (HCl) was used to adjust the pH. Samples at different ionic strengths were prepared with 0.05 and 0.1*M* potassium chloride (KCl) solutions.

Characterization

A Brookhaven dynamic light scattering apparatus was used to measure the particle size and particle size distribution over a period of time. The samples were placed in a decahydronaphthalene vat jacketed by a temperature-controlled water bath with a set point of 25°C. Light scattering experiments were then carried out with a 514.5-nm Coherent Inc. (Santa Clara, CA) Innova 90-5 argon-ion laser working at a constant power output of 200 mW. A Brookhaven Instruments (Holtsville, NY) photomultiplier detector tube (in photon counting mode) was kept at a fixed angle of 90° to the incident beam path, with a pinhole aperture size of 200 μm. For each sample, the time-dependent intensity fluctuation data was collected from the instrument and correlated with a BI 9000AT digital correlator (Brookhaven Instruments Corp.) over a delay range of 25 ns to 100 ms (with 342 channels plus 4 extended channels). Analysis of the autocorrelation function in terms of the particle size distribution was done numerically with a non-negatively constrained least squares (regularized CONTIN) method.

RESULTS AND DISCUSSION

In all of the particle size distribution plots that follow, the *x* axis represents the diameter of the particles in nanometers, and the *y* axis represents the population of particles corresponding to each diameter in terms of the intensity. For all experiments, coagulant was added at a time of 0 min at a concentration of 5 pph. For comparison, the particle size distribution of the neat latex (i.e., with no coagulant added) is also shown in all of the figures. As expected, the latex particles with no coagulant showed a monomodal size distribution with a mean diameter of 200–205 nm. The particle size distribution for each sample was initially measured 15 min after coagulant was added and every 5 or 10 min thereafter. For clarity, only size distributions from three select time points are shown in the following figures.

Figure 1 shows the evolution of the particle size distribution with time for samples of latex particles at pH 6 with two different particle concentrations, 10 and 15 wt %. The figure shows a broad size distribution for the aggregates. The particles started to aggregate within a few minutes of mixing. Figure 1(a) shows an increase in the mean diameter of the aggregates with time. The data collected at 15 and 20 min (not shown) showed a monomodal distribution with a mean diameter of about 500 nm. This population of aggregates persisted at later times. However, another interesting feature of the data that developed after about 35 min was a second mode of

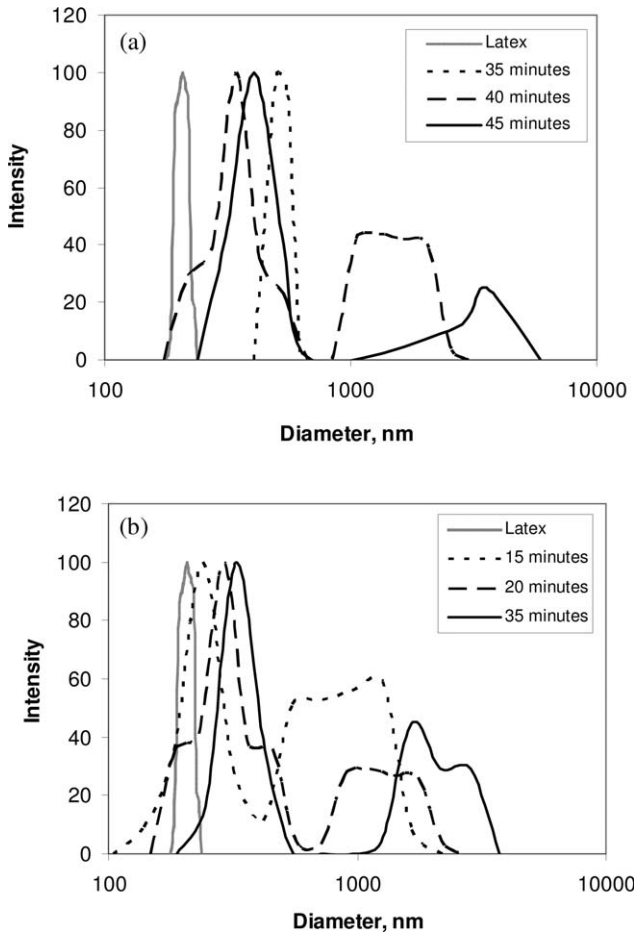

Figure 1 Particle size distribution at pH 6 for (a) 10 and (b) 15% latex suspensions in the presence of 5 pph of a cationic coagulant.

the distribution. Data taken at time points after 35 min showed a bimodal distribution, with one population of aggregates about 500 nm in diameter and a second population of aggregates with diameters ranging from 1000 to 10,000 nm. This suggests that after a certain amount of time, two different mechanisms for aggregate growth were present, one where existing aggregates grew slowly by the addition of individual particles or very small aggregates and a second one, whereby two large aggregates joined together to form very large clusters. Figure 1(b) shows similar behavior at a higher particle concentration; however, here, the bimodal nature of the distribution appeared almost immediately.

Figure 2 shows the particle size distribution for the colloidal suspensions at pH 2, prepared with buffer. Lowering the pH decreased the degree of ionization of the carboxyl groups on the particle surface, effectively decreasing the electrostatic repulsion between particles. Thus, we expected that this would increase the rate of aggregation. We did find some aggregation during the first 15–30 min after the coagulant was added, but it was not the dramatic increase in aggregation rate we expected on the basis of studies of the CPT process from the literature. The suspensions were allowed to stand overnight, and the data was collected after 15–16 h. As shown in Figure 2, aggregates with an average mean diameter of about 1000 nm were formed. The distributions themselves were monomodal and were slightly narrower than those obtained at pH 6; this suggests that the slower aggregation process allowed for some particle rearrangement within clusters to form more uniform aggregates.

In comparing these results with those taken at pH 6 (Fig. 1), we observed that the initial aggregation process was not affected; however, the formation of large clusters was significantly slowed. If our proposed mechanisms for aggregation are correct, this implies that the addition of individual particles onto clusters is not strongly pH-dependent, but that large clusters forming via the joining of large aggregates is unfavorable at low pH. The reason for this is unclear; we would expect that this mechanism would also be more favorable at low pH because the electrostatic repulsion between large aggregates

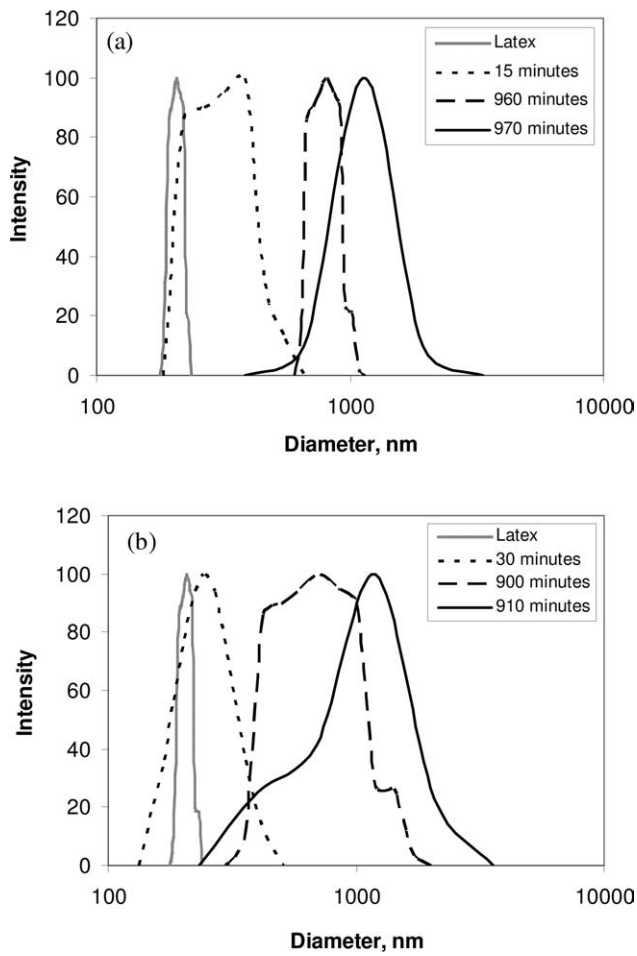

Figure 2 Particle size distribution at pH 2 (with buffer) for (a) 10 and (b) 15 wt % latex suspensions in the presence of 5 pph of a cationic coagulant.

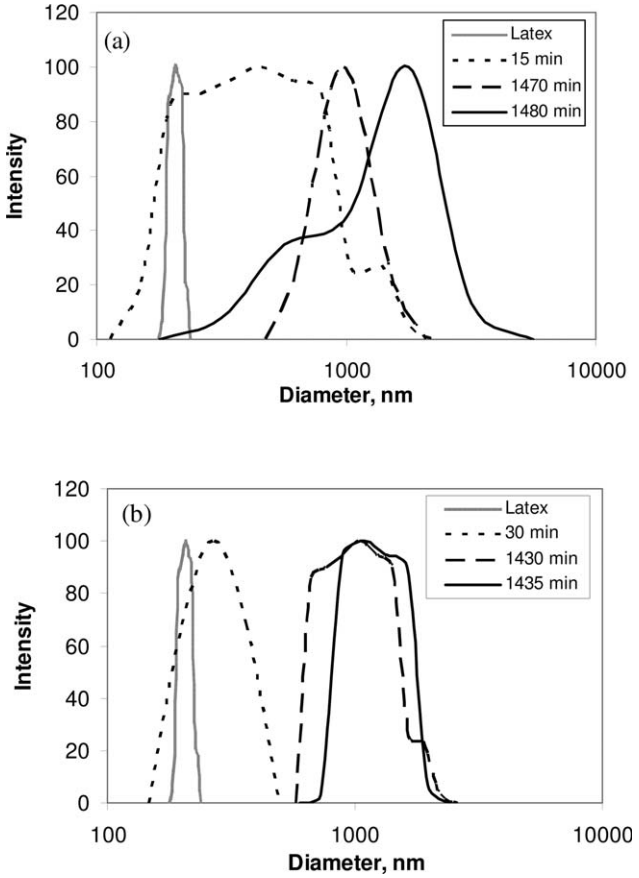

Figure 3 Particle size distribution at pH 2 (with HCl) for (a) 10 and (b) 15% latex suspensions in the presence of 5 pph of a cationic coagulant.

would also be smaller at pH 2 as compared to pH 6. It is possible that there were additional groups on the particle surface that were less stable at lower pH, which could have impacted the aggregation process. Experiments are underway with a more well-characterized model system to verify whether this pH effect was related to the chemistry of this specific system or whether it is more universal.

Samples prepared in buffer solutions have a large amount of added salt, which would contribute to the screening of electrostatic effects. To reduce the amount of added salt, we performed an additional set of experiments with the pH adjusted to 2 using HCl. It was observed that suspensions prepared with HCl showed the same behavior as the suspensions at pH 2 prepared from the buffer solution. Figure 3 shows the particle size distribution at pH 2 prepared with HCl for the 10 and 15% latex suspensions in the presence of 5 pph of the cationic coagulant. The data was quite similar to that taken at pH 2 with buffer, with some aggregation seen in the first 15–30 min, but no large aggregates formed until several hours later. The average mean diameter of the aggregates formed with time was, again, around 1000 nm, and the slower aggregation process appeared to result in more monodisperse aggregates. These data indicate that the aggregation process was not strictly electrostatic and supported our idea that there may have been some acid-sensitive surface chemistry on the primary particles that affected aggregation.

Another way to determine the role of electrostatics in the aggregation process is to increase the ionic strength of the samples independent of the pH by simply adding salt. As discussed previously, this may reduce the strength of attraction between particles by reducing the efficiency of the coagulant, but it will also screen the electrostatic repulsion between particles. Increasing the ionic strength of the suspension while holding pH = 6 did not appreciably slow the rate of aggregation but resulted in a broader aggregate size distribution, as seen in Figure 4 for a latex suspension with 10 wt % solids. Figure 4(a) shows the aggregation behavior for suspensions prepared with 0.05*M* KCl. The particles aggregated within few minutes, and an increase in the mean diameter of the aggregates with time was observed. Data acquired at 80 min showed a particle mean

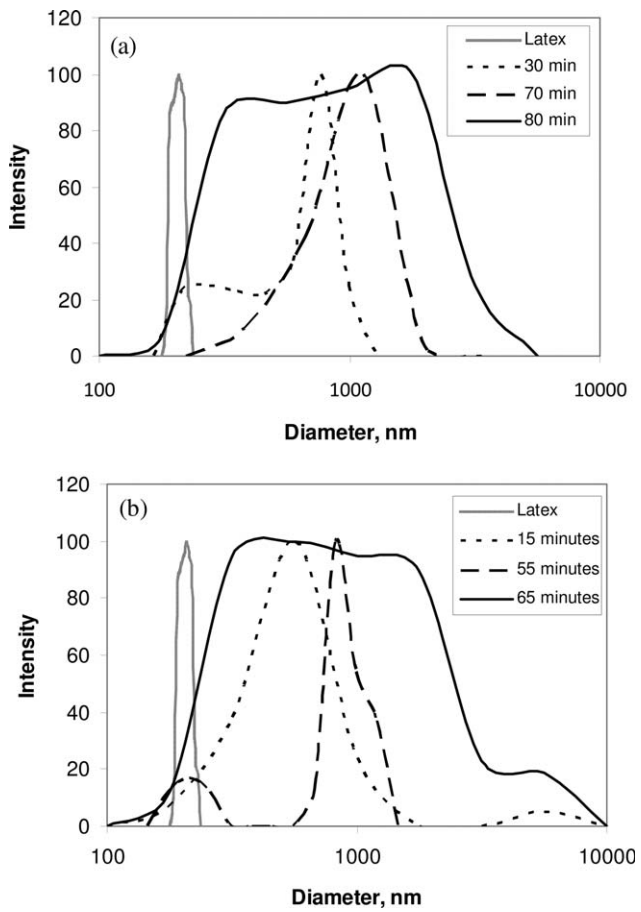

Figure 4 Effect of the ionic strength, (a) 0.05 and (b) 0.1*M* KCl, on the particle size distribution for a 10% latex suspension at pH 6 in the presence of 5 pph of a cationic coagulant.

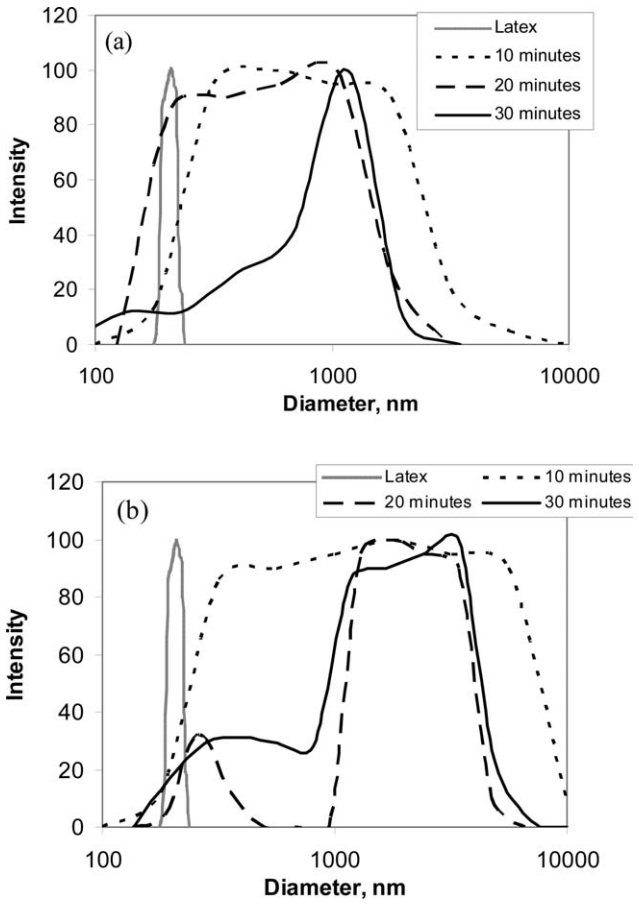

Figure 5 Particle size distribution at pH 6 for (a) 10 and (b) 15% latex suspensions in the presence of 5 pph of 10% aluminum sulfate.

diameter of 1000 nm, and data at 85 min showed a particle mean diameter of about 1400 nm. The suspension prepared with 0.1*M* KCl, as shown in Figure 4(b), showed a similar trend. Data acquired at 65 and 70 min showed particle mean diameters of about 1200 and 1500 nm, respectively. Increasing the ionic strength of the suspensions seemed to result in a slight increase in the average size of the aggregates, as the population of large aggregate sizes was higher in these samples as compared to Figure 1.

The results shown in Figures 1–4 used the commercial coagulant provided by Xerox. Figure 5 shows results from aggregation studies on suspensions at pH 6 with a model coagulant, aluminum sulfate. These systems also formed micrometer-sized aggregates within a few minutes. The aggregate size distribution seemed to be more polydisperse, and the mean diameter of the aggregates formed with time was in the range 1000–2000 nm. For the sample at 15 wt %, the system again showed the trend toward forming bimodal size distributions at longer times; this suggested that perhaps the two different aggregation mechanisms proposed previously also played a role in this system. The distributions at 10 wt % were so broad that it was difficult to determine if this trend was also present in these systems. The samples prepared for the study were allowed to stand overnight, and the data was acquired after 26 h. There was no appreciable increase in the aggregate size after this time. This indicated that the aggregation process reached some stable size within 30–40 min.

CONCLUSIONS

We investigated the effect of the pH and ionic strength on aggregation in systems that mimicked the EA process for toner production. With a commercial coagulant, it was found that the aggregation process eventually slowed and stopped in these systems; this led to finite-sized aggregates with sizes of about 1000 nm. This was in contrast to the infinite fractal aggregates that are typically formed by attractive colloids. At longer times, a bimodal distribution was formed; this suggested that there may have been two different aggregation mechanisms occurring. Somewhat surprisingly, we found that lowering the pH of the samples slowed down the aggregation process considerably, in contrast to the conventional CPT process, where lowering the pH triggers fast aggregation. However, we did not observe a similar slowing of aggregation in samples at neutral pH with added salt. The addition of salt resulted in slightly broader aggregation size distributions. We suspect that the aggregation process was not completely controlled by electrostatics and that there may have been some surface groups on the particles that were acid sensitive. We are currently performing experiments with more well-characterized particles to verify this trend. We also studied the particle size distribution for the latex suspensions using a 10% aluminum sulfate solution as a model coagulant, and these systems showed similar trends as the commercial system; this suggested that this system may serve as a good model for the industrial system.

References

1. Gruber, R. J.; Julien, P. C. Handbook of Imaging Materials; Diamond, A. S., Ed.; Marcel Dekker: New York, 1991; p 159.
2. Maekawa, H.; Hisamatsu, K.; Emura, Y.; Ogawa, K.; Mizushima, K. (to Mitsui Chemicals, Inc.) Eur. Pat. EP 1011031 A1 (2000).
3. Ding, P.; Pacek, A. W.; Abinhava, K.; Pickard, S.; Edwards, M. R.; Nienow, A. W. Ind Eng Chem Res 2005, 44, 6004.
4. Ding, P.; Pacek, A. W.; Abinhava, K.; Pickard, S.; Edwards, M. R.; Nienow, A. W. Ind Eng Chem Res 2005, 44, 6012.
5. Ahuja, S.; Lai, Z.; Cheng, C. (to Xerox Corp.) U.S. Pat. US20070207400 (2007).
6. Lai, Z.; Fong, R.; Tong, Y.; Cheng, C.; Grillo, A.; Smith, P.; Gerroir, P.; Ong, B. (to Xerox Corp.) U.S. Pat. US20080063965 (2008).

7. Dimon, P.; Sinha, S. K.; Weitz, D. A.; Safinya, C. R.; Smith, G. S.; Varady, W. A.; Lindsay, H. M. Phys Rev Lett 1986, 57, 595.
8. Gisler, T.; Ball, R.; Weitz, D. A. Phys Rev Lett 1999, 82, 1064.
9. Kolb, M.; Jullien, R. J Phys Lett Paris 1984, 45, L977.
10. Schaefer, D. W.; Martin, J. E.; Wiltzius, P.; Cannell, D. S. Phys Rev Lett 1984, 52, 2371.
11. Osuji, C. O.; Kim, C.; Weitz, D. A. Phys Rev E 2008, 77, 060402.
12. Lu, P. J.; Zaccarelli, E.; Ciulla, F.; Schofield, A. B.; Sciortino, F.; Weitz, D. A. Nature 2008, 453, 499.
13. Sciortino, F.; Mossa, S.; Zaccarelli, E.; Tartaglia, P. Phys Rev Lett 2004, 93, 055701.
14. Lu, P. J.; Conrad, J. C.; Wyss, H. M.; Schofield, A. B.; Weitz, D. A. Phys Rev Lett 2006, 96, 028306.